Materials and Structures, 1994, **27**, 79–90

Failure of slender and stocky reinforced concrete columns: tests of size effect

Z. P. BAŽANT, Y. W. KWON*

Department of Civil Engineering, Northwestern University, Evanston, IL 60208, USA

The paper reports the results of a series of tests of geometrically similar pin-ended tied reinforced concrete columns of different sizes, with ratio 1:2:4, and slendernesses of 19.2, 35.8 and 52.5. The model columns had square cross-sections of sides 0.5, 1 and 2 in. (12.7, 25.4 and 50.8 mm), reduced-size steel bars with steel ratio 4.91%, and reduced-size aggregate with maximum size 1/8 in. (3.2 mm). The axial load was eccentric, with end eccentricities 0.25 of the cross-section side. It is found that for all slendernesses the failure loads exhibit a strong size effect in which the nominal stress at maximum load (load divided by cross-sectional area) decreases as the size is increased. This contradicts the current design codes, which exhibit no size effect, and indicates that the failure is governed by fracture mechanics. The results are in good agreement with the size-effect law previously proposed by Bažant. For a higher slenderness, the size effect increases and the brittleness of failure, characterizing the proximity to the behaviour described by linear elastic fracture mechanics, increases. The role of bond slip in the observed size effect remains to be clarified.

1. INTRODUCTION

One basic characteristic of material failure criteria expressed in terms of strength or yield surface, or implied by constitutive relations in terms of stresses and strains, is that there is no effect of the size of the structure on its nominal strength. The current design codes including the ACI code, are based on the theory of limit states, justified by the theory of plasticity, which implies that the code provisions for ultimate loads in all types of failure exhibit no size effect. However, the fact that the observed load–deflection diagrams of columns descend after the peak, rather than terminating with a horizontal yield plateau, invalidates the use of the theory of limit states [1].

As is now clear, concrete is not plastic but brittle and its description in terms of plasticity is in principle incorrect (except for behaviour under confining pressures that greatly exceed the uniaxial compression strength). The behaviour of concrete is characterized by post-peak strain softening which is due to progressive development of damage in the form of microcracks and localization of such microcracks into a major crack that leads to the final failure. Mathematical modelling of such behaviour must be based on fracture mechanics, the characteristic attribute of which is that the material model is not completely describable in terms of stress and strain (or strength, or yield limit). Rather, the material model must also involve an energy quantity, called the fracture energy, or equivalently a length quantity, called the characteristic length, which is a material property. Such a material model predicts a size effect, such that the nominal stress at failure, σ_N, decreases with the characteristic dimension of the structure, D, if geometrically similar structures of different sizes are compared.

After great advances in fracture mechanics of concrete during the last decade, it is now clear that such size effects must occur in all the failures of concrete structures that are due to concrete rather than steel. This is true not only of those failures which are due to concrete failing in tension (diagonal shear, punching shear, torsion, bar pull-out, anchor pull-out, splice failure, etc.) but also of all the failures which are due to concrete failing in compression. This includes prestressed concrete beams and, most importantly, reinforced concrete columns, whose study from the size-effect viewpoint is the purpose of this article.

The material fracture properties are not the only reason why a size effect must be expected to occur in reinforced concrete columns. After the research of the last decade, it is now also known that if the load–deflection diagram of a structure exhibits post-peak softening, and if the softening is not explicable by non-linear geometric effects (in columns the so-called P–Δ effects), then in general the post-peak softening response exhibits a size effect, and so does the nominal strength (except when the structure behaves according to the series coupling model). Now, it is known from experiments that the load–deflection diagram of reinforced concrete columns, even short ones in which the P–Δ effect is negligible, exhibits post-peak softening. Hence, a size effect ought to exist. The objective of this paper is to demonstrate it by experimental results (on which a preliminary, abbreviated report has been given at a recent conference [2]).

Although important advances have been made in the past in understanding the behaviour of reinforced concrete columns (see e.g. Nilson and Winter [3] and for

* On leave from Inchon University, Seoul, Korea.

0025-5432/94 © RILEM

further references consult McGregor [4], Bažant and Cedolin [5] and Bažant *et al.* [6]), the size effect in columns has escaped attention so far. But no phenomenon in physics is understood until the scaling law is understood. This also applies to concrete structures. Discrepancies in the scaling laws at very large and very small distances were the primary impulse for the development of the theories of relativity and quantum mechanics, and the scaling problems of fluid mechanics led to boundary-layer theory and the theory of turbulence [7].

Until about ten years ago, it had been erroneously believed that all the size effects in concrete structures are totally explicable by the statistical nature of material strength, as described by Weibull-type theories, and that they should therefore be relegated to safety factors and left to probabilists to worry about. In reality, however, the portion of the size effect ascribable to the randomness of concrete strength is very small and negligible in structures in which there is large crack growth before the maximum load is reached [8–10]. In such structures, the size effect is almost totally deterministic and is caused by the fact that a larger structure stores a greater amount of strain energy and thus releases more energy into an advancing fracture front, while the energy dissipated at the fracture front per unit fracture advance is approximately independent of the structure size.

2. EXAMPLES OF LACK OF SIZE EFFECT IN STRENGTH THEORY

It might be useful to begin by simple examples illustrating that indeed the column design procedures based on the concept of strength or yield exhibit no size effect, i.e. $\sigma_N = P/bD$ = constant for geometrically similar columns of different sizes D where P = maximum load; b, D = height and width of rectangular cross-section. As one example, considering a perfect slender homogeneous (i.e. unreinforced) centrically loaded column made from a deterministic elastic material, we have, according to Euler's formula,

$$\frac{P}{bD} = \sigma_N = \sigma_{cr} = \pi^2 E \frac{r^2}{L^2} \qquad r = \frac{D}{(12)^{1/2}} \tag{1}$$

where E = Young's elastic modulus, L = effective column length and r = cross-section radius of gyration. Here obviously σ_N = constant since L/r and L/D are constant for geometrically similar columns.

As another example, consider a homogeneous hinged column of sinusoidal initial curvature with initial load eccentricity e at mid-span. From the theory of bending, the maximum stress in the column is $\sigma_{NM} = \sigma_N + 6Pz/bD^2$ where $z = e/[1 - (P/P_{cr})]$ and $P_{cr} = \pi^2 EbD^3/12L^2$ = Euler load. This yields

$$\sigma_{NM} = \frac{P}{bD}\left(1 + \frac{6e}{D[1 - (12/\pi^2 E)(L^2/D^2)(P/bD)]}\right) \tag{2}$$

Setting σ_{NM} = constant = f'_c and solving for P, we again see that, for geometrically similar columns, $\sigma_N = P/bD$ is constant, independent of structure size D. Similarly it can be demonstrated that the ACI column design procedure gives the same value of P/bD for all geometrically similar columns, both for three-dimensional similarity, for which b is proportional to D, as is the present case, and for two-dimensional similarity, for which b is constant.

These examples illustrate that if there is a size effect, it cannot be described by means of the classical theory. Therefore, tests of the effect of structure size are the best way to decide whether the classical theory is valid. With this motivation, the test programme described in the following has been carried out.

3. EXPERIMENTAL PROCEDURE

The test specimens (Fig. 1) were tied reinforced concrete columns of square cross-sections with sides D = 0.5, 1 and 2 in. (12.7, 25.4 and 50.8 mm). Three column slendernesses λ = 19.2, 35.8 and 52.5, were used: $\lambda = L/r$ and according to ACI, $r = 0.3D$ (for typical reinforced concrete cross-sections). The corresponding effective lengths L of the columns, measured between the contact points of the steel balls (Fig. 1), were L = 2.875, 5.375 and 7.875 in. (73, 136.5 and 200 mm) for the smallest cross-section, L = 5.75, 10.75 and 15.75 in. (146, 273 and 400 mm) for the middle cross-section, and L = 11.5, 21.5 and 31.5 in. (292, 546 and 800 mm) for the largest cross-section. The corresponding net lengths of the columns without the support plates but with the steel

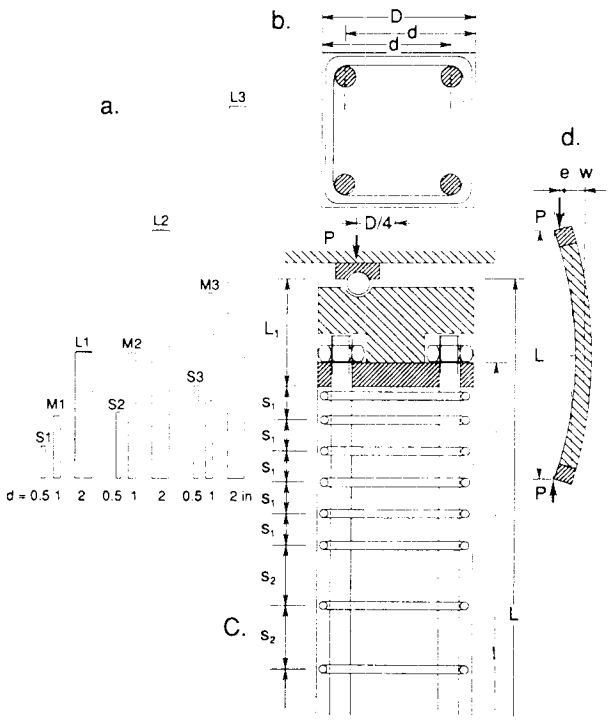

Fig. 1 (a) Side view of test columns of different sizes, (b) cross-section, (c) vertical cross-section through the column and load application, (d) measurement of lateral deflection.

cover plates (Fig. 1) were $l = 2.5$, 5 and 7.5 in. (63.5, 127 and 190.5 mm) for the smallest cross-section, $l = 5$, 10 and 15 in. (127, 254 and 381 mm) for the middle cross-section, and $l = 10$, 20 and 30 in. (254, 508 and 762 mm) for the largest cross-section. The loads were applied to the steel platens through steel balls and steel plates.

The columns of each group of the same slenderness and different cross-sections were geometrically similar (Fig. 1b). The geometric similarity was enforced scrupulously: the reinforcing bars, their locations and cover, as well as the diameter and spacing of the ties were all scaled in proportion to D. Thus the thickness of the concrete cover of longitudinal bars, measured from the bar centre to the surface, was not constant, but was $d_c = 0.2D$. Because of the unavailability of deformed reinforcing bars of sufficiently small diameter, smooth steel bars had to be used for both the main bars and the ties, in order to achieve geometric similarity. To limit the possibilities of bond slip, the column ends were provided with cover plates (Fig. 1c) at which the vertical bars were anchored by threaded nuts fitting into bores in massive end-platens (Fig. 1c), which were also geometrically scaled (in retrospect, though, it must be admitted that the nuts could not have prevented the bars from being pushed out of the column end, nor from slipping farther from the ends, although no observations were made on whether this actually happened).

The columns were simply supported, and the load P was applied with eccentricities e which were geometrically similar: $e = 0.25D$. The steel ratio was 4.91%. Each column had four longitudinal bars as shown in Fig. 1b, of diameters $d_b = \frac{1}{16}$, $\frac{1}{8}$ and $\frac{1}{4}$ in. (1.59, 3.18 and 6.35 mm) for the smallest, middle and largest column sizes, respectively. The corresponding diameters of the steel ties were $\frac{1}{32}$, $\frac{1}{16}$ and $\frac{1}{8}$ in. (0.79, 1.59 and 3.18 mm). The ties were glued by epoxy to the four main bars and had overlap splices at the corners. The spacing of the ties (centre to centre) was 0.3, 0.6 and 1.2 in. (7.62, 15.2 and 30.5 mm) for the smallest, middle and largest cross-sections, but near the ends the spacings were reduced to 0.2, 0.4 and 0.8 in. (5.08, 10.2 and 20.3 mm) respectively, and very near the ends to 0.1, 0.2 and 0.4 in. (2.54, 5.08 and 10.2 mm), respectively (see Fig. 1c).

The Young's modulus of the steel bars was $E_s = 29\,000$ ksi (200 GPa) and the yield strength was $f_y = 80\,000$ psi (552 MPa). This value of yield strength was only slightly higher than the highest yield limit of the bars currently in wide usage, which is 75 000 psi (517 MPa). The compressive steel stress calculated for the ultimate load state of the least slender test column with eccentricity $D/4$ is 63 770 psi (440 MPa), and for the cases of more slender columns, this value is even less.

The concrete (actually a microconcrete or mortar) was made of Type I Portland cement with water/cement ratio 0.65 (for easy workability) and aggregate/cement ratio 2.5 (by weight). The aggregate used in the mix was an air-dried siliceous sand of maximum grain size 0.132 in. (3.35 mm), passing through sieve No. 6. All specimens were cast from the same batch of concrete. The average uniaxial compression strength was $f'_c = 4200$ psi (28.96 MPa); it was measured on 28-day-old companion cylinders of diameter 3 in. (76.2 mm) and length 6 in. (152.4 mm), which were all cast from the same batch of concrete as the specimens, cured in the same manner as the columns, and tested at the same age right after removal from the moist room.

The columns were cast in forms made of plywood with a smooth and hard varnish-painted surface. The forms were stripped after one day, after which the columns, as well as the companion cylinders, were cured until 28 days of age in a water bath at 20°C. At the age of 28 days, the columns were tested in a closed-loop (MTS) testing machine. The lateral deflection at the mid-height of the column was measured by an LVDT gauge (Fig. 1d). The stroke rate in each test was controlled to be kept constant and was chosen so as to reach the peak load, for any column size and slenderness, within about 15 min. Since the specimens were tested right after being taken from the moist room, they have not experienced before the test any appreciable drying, and thus no cracking damage and no size effect due to drying shrinkage could have occurred.

Typical photographs of the broken columns are shown in Figs 2–7. Although the present evaluation of the tests does not require detailed pictures of the failure surfaces, they will be important to any analyst trying to simulate these failures and the size effect by finite elements or other sophisticated numerical methods. Many of the columns broke right at mid-length, as might be expected from buckling analysis. However, the small slender columns underwent asymmetric breaks – about half of them near

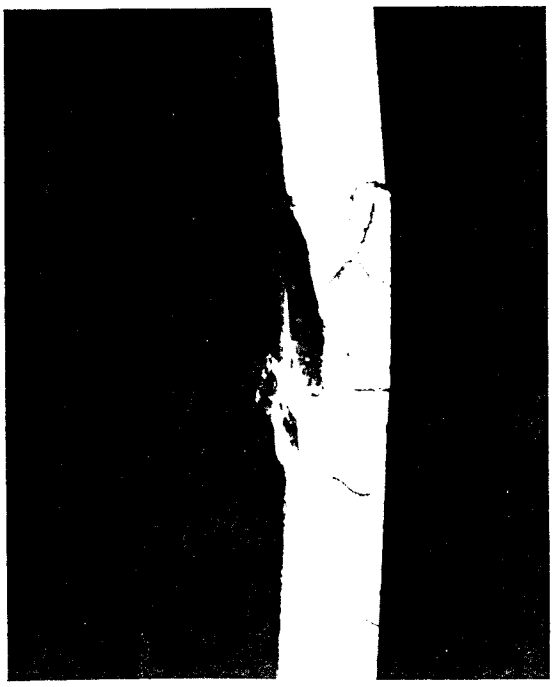

Fig. 2 Typical break of the column.

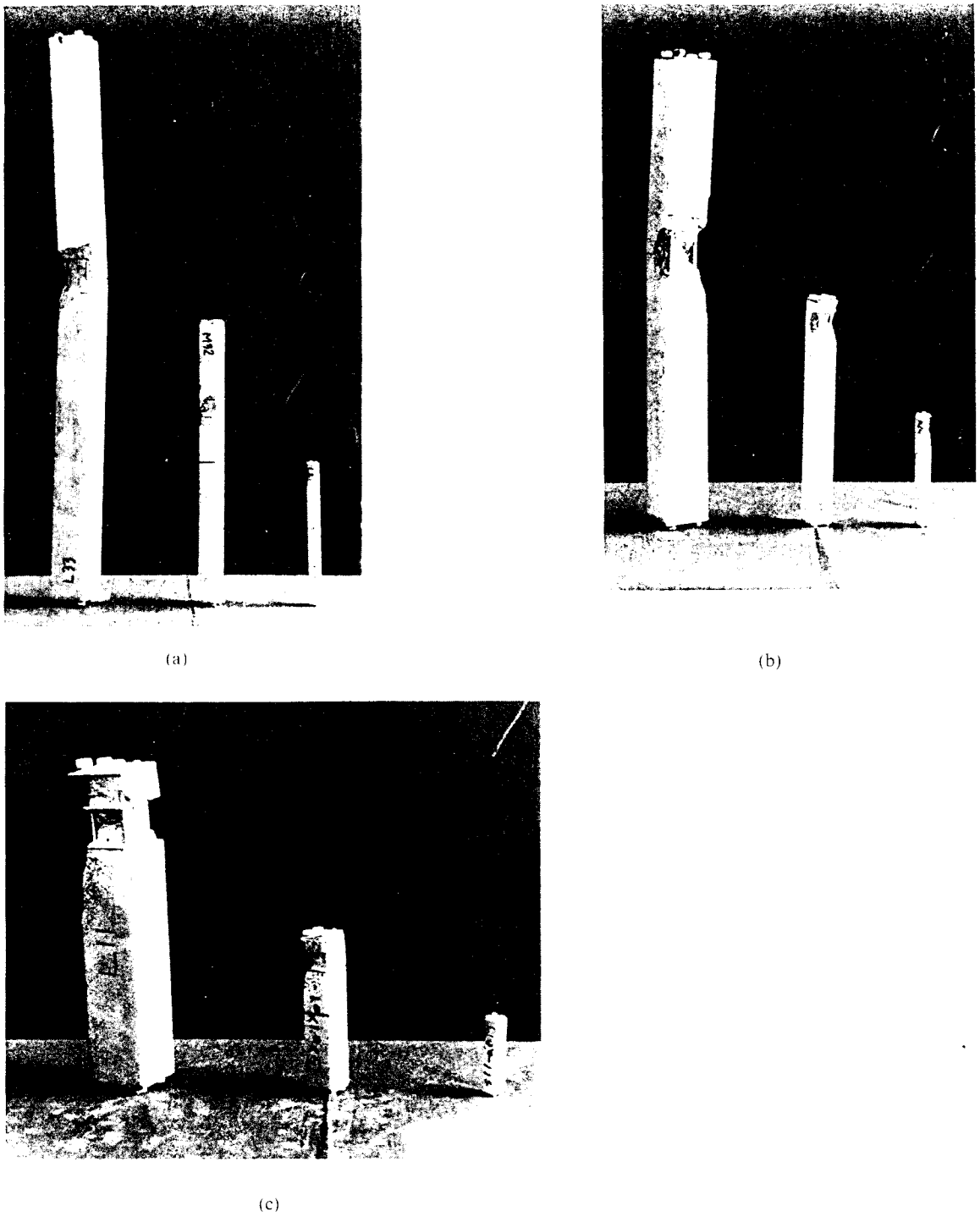

Fig. 3 Similar columns of all three sizes: (a) slender, (b) medium, (c) stocky.

the quarter-length and the other half all the way at one end, upper or lower.

Assuming the break to be caused by the bending moment, it might at first seem hard to understand how the columns can break at the end. The fact that many of them do is a manifestation of the fact that the failure cannot really be caused by the bending moment. From the fracture mechanics viewpoint, the failure ought to be caused by the release of stored strain energy engendered by the compression fracture, which leads to unloading due to axial extension of the elastic part of the specimen. Thus the fracture causes the release of the stored bending energy regardless of whether the fracture happens at mid-length or near the ends of the column. The larger

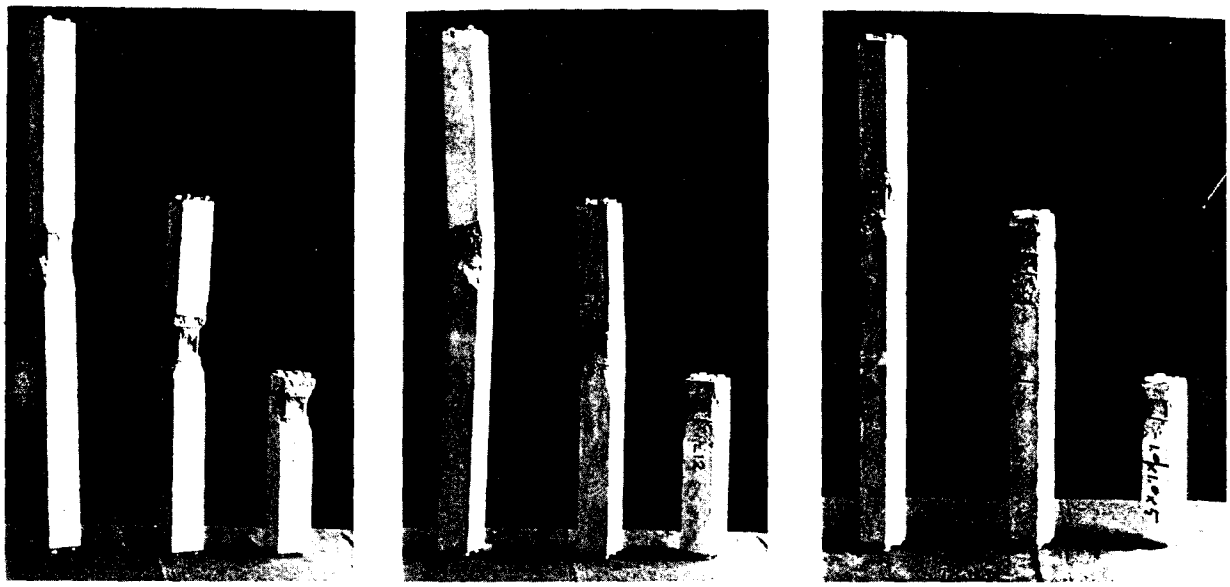

(a) (b) (c)

Fig. 4 Columns of all three slendernesses: (a, b) large size, (c) medium size.

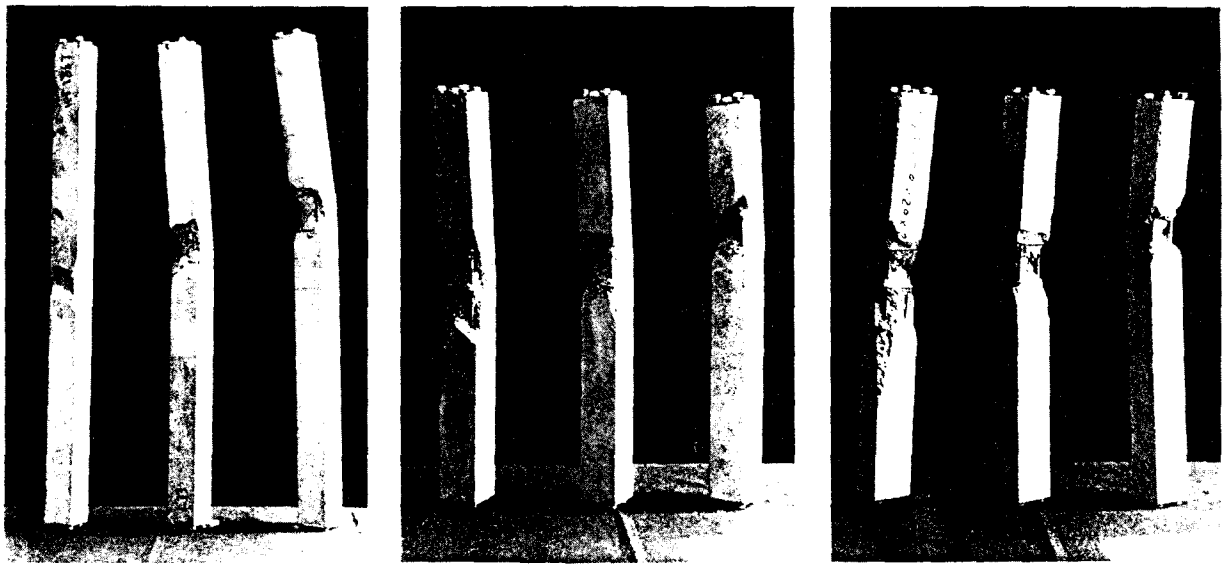

(a) (b) (c)

Fig. 5 Sets of identical columns: (a) large and high slenderness; (b, c) large and medium slenderness.

bending moment at the mid-length of course promotes the start of the fracture at mid-length, but the same argument cannot be made for the energy release, while at the same time the inevitable stress concentrations under the end cover-plates promote a start of fracture near the ends. The strength, of course, matters only for the initiation of fracture, not for its subsequent growth. The fracture growth is governed mainly by energy release of the structure. The fracture process may initiate simultaneously at the mid-length and near the end but (because of the well-known localization instability) the fracture can grow only at one place.

There could be, however, also another reason for fracture near the ends: failure of bond, i.e. slip between steel bars and concrete. The fact that smooth bars were used and the ties were glued rather than welded to the longitudinal bars may have made the slip possible. If the stress–displacement diagram for the interface slip involves softening, then the slip alone could have caused some part of the size effect.

(a) (b) (c)

Fig. 6 Sets of identical columns: (a) medium size and slender: (b, c) medium size and medium slenderness.

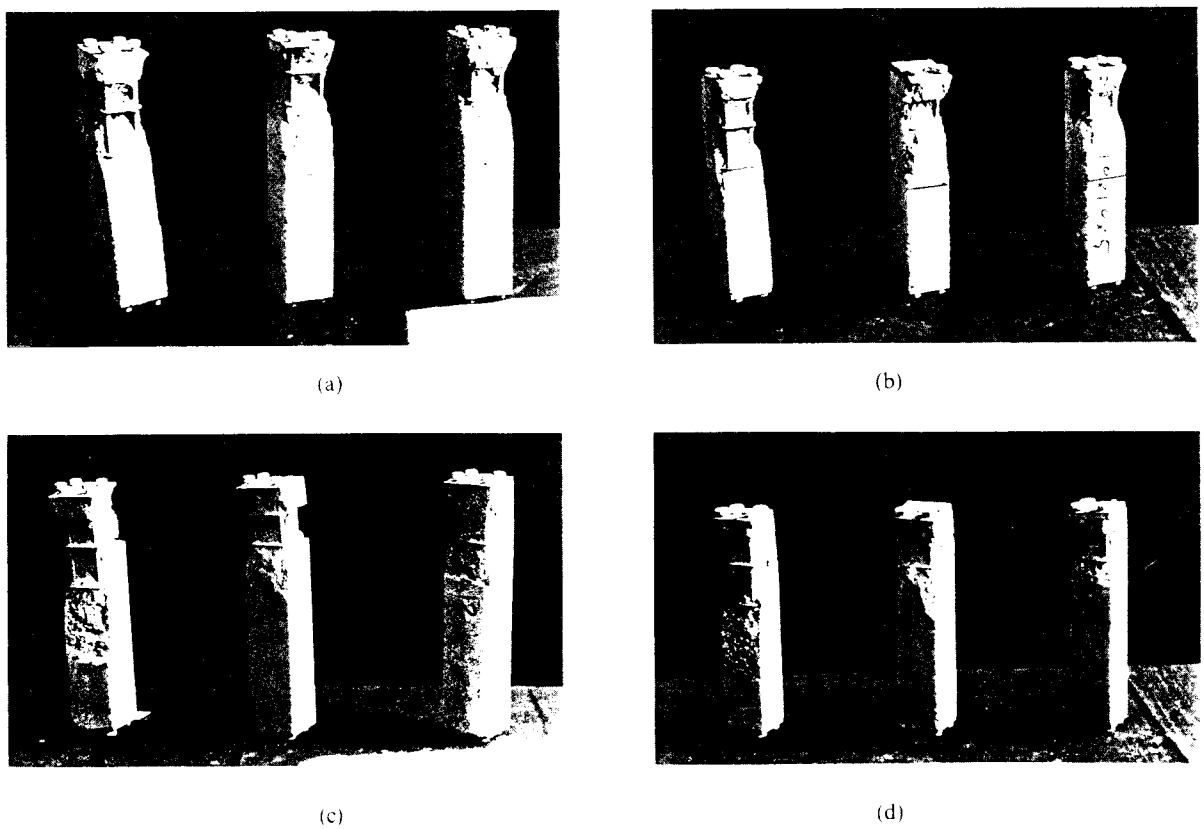

(a) (b)

(c) (d)

Fig. 7 Sets of identical columns: (a, b) large size and stocky; (c, d) medium size and stocky.

4. RESULTS

The test results are summarized in Table 1, which shows the load values in kip (1 kip = 1000 lbf = 4448 N) and the corresponding lateral deflections at mid-span (in inches). For each column, the measurements are reported for one pre-peak state on the ascending branch, the peak load (maximum load) state and one post-peak state on the descending branch. In the specimen labels, S, M and L mean the small, middle and large cross-section; the

Table 1 Measured axial load P and mid-height deflection w for various column slendernesses λ and cross-section sizes D

D	λ	Specimen	Pre-peak state		Peak load state		Post-peak state	
			P (kip)	w (in.)	P (kip)	w (in.)	P (kip)	w (in.)
0.5	19.2	S1-1	0.205	0.005	1.03	0.025	0.208	0.118
		S1-2	0.202	0.009	0.83	0.023	0.200	0.011
	35.8	S2-1	0.203	0.014	0.86	0.044	0.24	0.14
		S2-2	0.205	0.025	0.80	0.063	0.20	0.14
		S2-3	0.208	0.024	0.70	0.055	0.26	0.08
	52.5	S3-1	0.208	0.019	0.875	0.085	0.20	0.149
		S3-2	0.205	0.019	0.807	0.087	0.20	0.171
		S3-3	–	–	0.566	0.093	–	–
1.0	19.2	M1-1	1.015	0.031	2.76	0.049	1.00	0.163
		M1-2	1.02	0.049	2.93	0.023	1.00	0.179
		M1-3	1.02	0.011	2.32	0.038	1.00	0.105
	35.8	M2-1	1.01	0.045	2.62	0.095	1.00	0.230
		M2-2	1.01	0.028	2.83	0.090	1.00	0.203
		M2-3	1.01	0.021	2.82	0.079	1.00	0.195
	52.5	M3-1	1.01	0.0302	2.49	0.148	1.01	0.370
		M3-2	1.02	0.038	2.37	0.165	1.00	0.377
		M3-3	1.00	0.050	2.47	0.188	1.03	0.252
2.0	19.2	L1-1	2.00	0.0068	10.85	0.0869	2.10	0.0346
		L1-2	2.00	0.0048	10.67	0.0767	4.16	0.276
		L1-3	2.02	0.015	10.53	0.0625	2.00	0.371
	35.8	L2-1	2.00	0.010	9.42	0.244	2.07	0.980
		L2-2	2.05	0.015	9.21	0.227	2.00	0.885
		L2-3	2.00	0.012	8.04	0.098	2.00	0.203
	52.5	L3-1	2.00	0.016	7.38	0.360	2.00	0.902
		L3-2	2.00	0.006	7.02	0.298	2.00	0.657
		L3-3	2.00	0.002	7.64	0.284	2.32	1.000

1 kip = 1000 lbf = 4448 N, 1 in. = 25.4 mm.

subsequent numbers, 1, 2 and 3 mean the low, middle and higher slenderness, respectively, and the numbers 1, 2 and 3 following a hyphen are the numbers of individual specimens.

Three identical specimens were tested for all cases except S1. The loads and deflections measured in individual tests are given in Table 1. The interaction diagram of maximum (ultimate) axial load P versus the corresponding bending moment M has been calculated according to the standard procedure described in concrete design textbooks (e.g. Nilson and Winter [3], McGregor [4] and McGregor *et al.* [11]). To be able to compare the columns of different sizes, we plot in Fig. 8 instead of P and M the non-dimensional load p and the non-dimensional moment m:

$$p = \frac{\sigma_N}{f'_c} = \frac{P}{D^2 f'_c} \tag{3}$$

$$m = \frac{\sigma_N}{f'_c}\left(\frac{e+w}{D}\right) = \frac{P(e+w)}{D^3 f'_c} \tag{4}$$

where P = measured load, w = measured mid-height deflection, $f'_c = 4200$ psi (28.96 MPa) = compression strength of concrete measured on the aforementioned companion cylinders, and $\sigma_N = P/D^2$ = nominal stress. If the code procedure is used (or if any strength or yield criteria are used) and if the cross-sections are geometrically similar, the interaction diagrams of p versus m are independent of the size D (as well as of the f'_c value). Thus the effect of D in this kind of plot directly reveals the size effect. The interaction diagram calculated according to ACI Code, which exhibits no size effect, is in this plot shown by the solid line in Fig. 8. Also shown (as the dashed line) is the interaction diagram that is scaled down according to the capacity reduction factors ϕ specified in ACI Code; $\phi = 0.7$ for axial compression with bending and $\phi = 0.9$ for pure flexure without axial load, with a linear transition of ϕ from 0.9 to 0.7 between $P = 0$ and the eccentricity for the balanced condition. The ϕ factors take into account material randomness.

Fig. 8a, b and c show the measured maximum load data for the individual specimens of the small, medium and

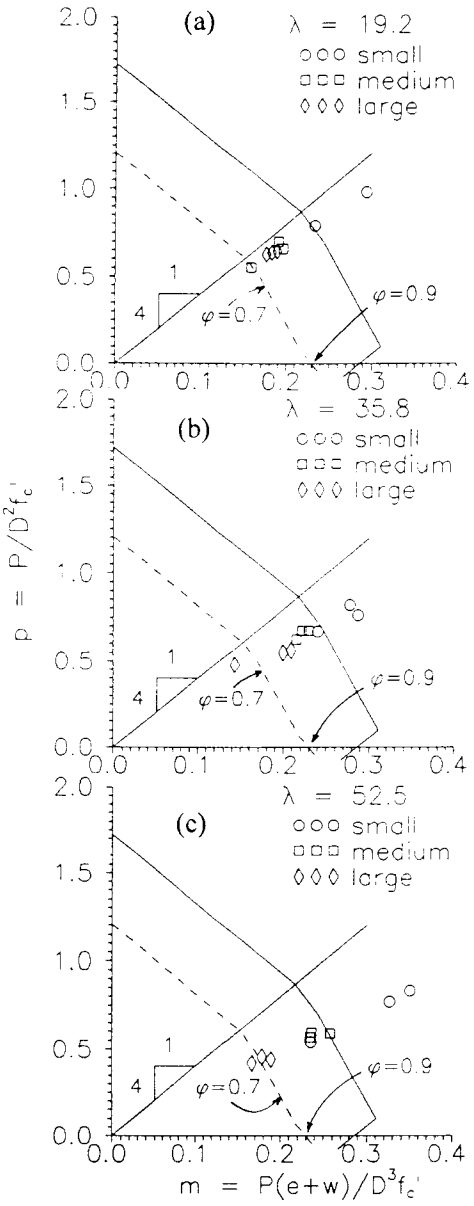

Fig. 8 Interaction diagram of axial load versus bending moment calculated from ACI code and individual test results at maximum load, for (a) small, (b) medium and (c) large slenderness.

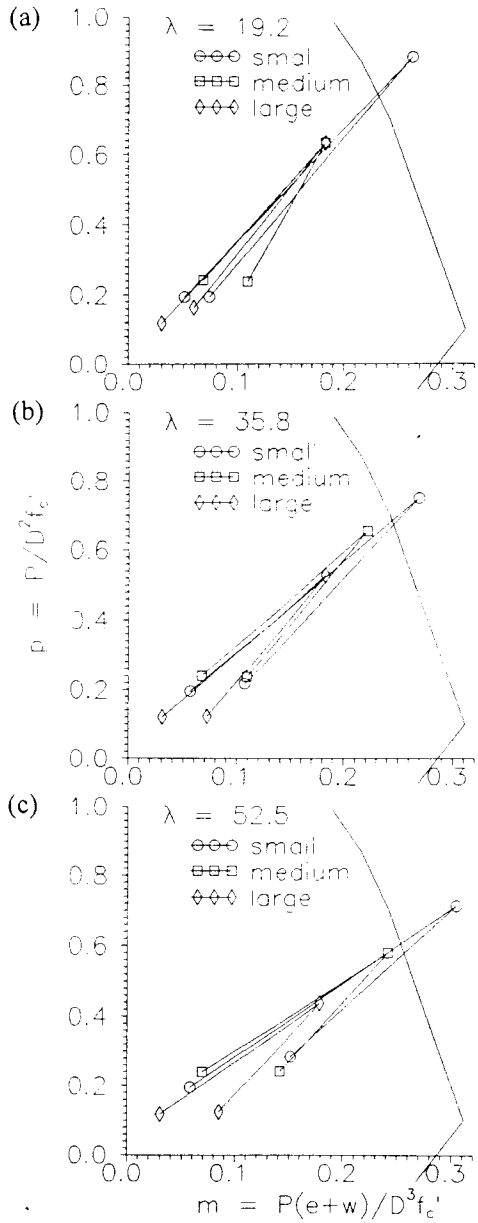

Fig. 9 Loading paths in interaction diagrams for various sizes and (a) small, (b) medium and (c) large slenderness.

large slendernesses, respectively. Each figure shows these data for the small, middle and large sizes.

In Fig. 9a, b and c the data points represent the measured loads and the corresponding bending moments at mid-length which are based on the measured deflections and include the buckling (slenderness) effects. In these figures, only the averages of each group of identical specimens are shown. In addition to the maximum load state, each figure also shows the pre-peak and post-peak states, and each line connecting these states represents the loading path in the interaction diagram.

For more slender columns, as expected, the response path moves to the right and describes a wider loop. The scatter of the data, as seen from Fig. 9, is normal for concrete testing.

5. DISCUSSION

The most interesting aspect of the test results is that, with increasing size, the data points systematically move towards the origin of the interaction diagram. Thus the experiments prove the existence of a size effect, as theoretically expected. This, of course, disagrees with the

existing design codes. When geometrically similar columns of different sizes, made of the same concrete, are considered, the codes predict the same nominal strength $P\,D^2$, the same non-dimensional load p, and the same non-dimensional moment m. Moreover, as we see, the size effect is quite significant. In fact, for some of the largest columns, the code predictions are even unsafe since the data point for the small slenderness lies within the short-column interaction diagram scaled down by the ϕ factor. The objective of a good design code is to provide uniform safety margins for various cases, but according to the present test results this is not achieved.

To further illuminate the size effect, let us plot log σ_N versus log D, which represents the standard size-effect plot. Such plots are given in Fig. 10a, b and c, in which the data points show, separately for each slenderness, the value of nominal strength $\sigma_N = P\,D^2$ calculated from the peak loads measured in individual tests. The data points in Fig. 11 represent the mean σ_N value for each group of identical specimens, and the plots for all the slendernesses are gathered in the same figure. All these plots clearly indicate a strong size effect. But according to the current code procedure, all these plots are obtained as horizontal lines. Furthermore, we see that the transition size D_0, obtained as the intersection of the horizontal and inclined asymptotes, shifts to the left (i.e. to smaller sizes) as the slenderness increases, making the size effect more pronounced.

Based on previous theoretical arguments of general validity (see Bažant and Cedolin [5], Chapters 12 and 13, or Bažant and Kazemi [12]), the size effect should be described by the following approximate size-effect law proposed by Bažant [8]:

$$\sigma_N = Bf'_t(1+\beta)^{-1/2} \qquad \beta = D/D_0 \tag{5}$$

in which Bf'_t and D_0 are two empirical constants (the tensile strength f'_t, estimated as $57\,000(f'_c)^{1/2}$, is introduced merely for convenience, to make B non-dimensional). The optimal fits by this size-effect law are shown in Figs 10 and 11 by the solid curves. For small sizes these curves approach a horizontal asymptote, and for large sizes they approach an inclined asymptote of slope $-\frac{1}{2}$, which corresponds to linear elastic fracture mechanics.

One aspect of Fig. 11 must be emphasized: for a more slender column, the response lies closer to the linear elastic fracture mechanics asymptote, i.e. the column is more brittle. This is not surprising, since a slender column stores more energy than a stockier column of the same cross-section. The brittleness has previously been characterized by the so-called brittleness number, $\beta = D/D_0$ [13, 14]. The point $\beta = 1$ (i.e. $D = D_0$) corresponds to the intersection of the horizontal and inclined asymptotes in Figs 10 and 11. From the test data we see that, for the smallest slendernesses, $\beta < 1$, while for the largest slenderness, $\beta > 1$.

Doubtless the size effect will be mitigated by stronger and more densely spaced ties. The reason is that increase of the triaxial confining pressure engendered by the ties causes concrete to become less brittle and less prone to

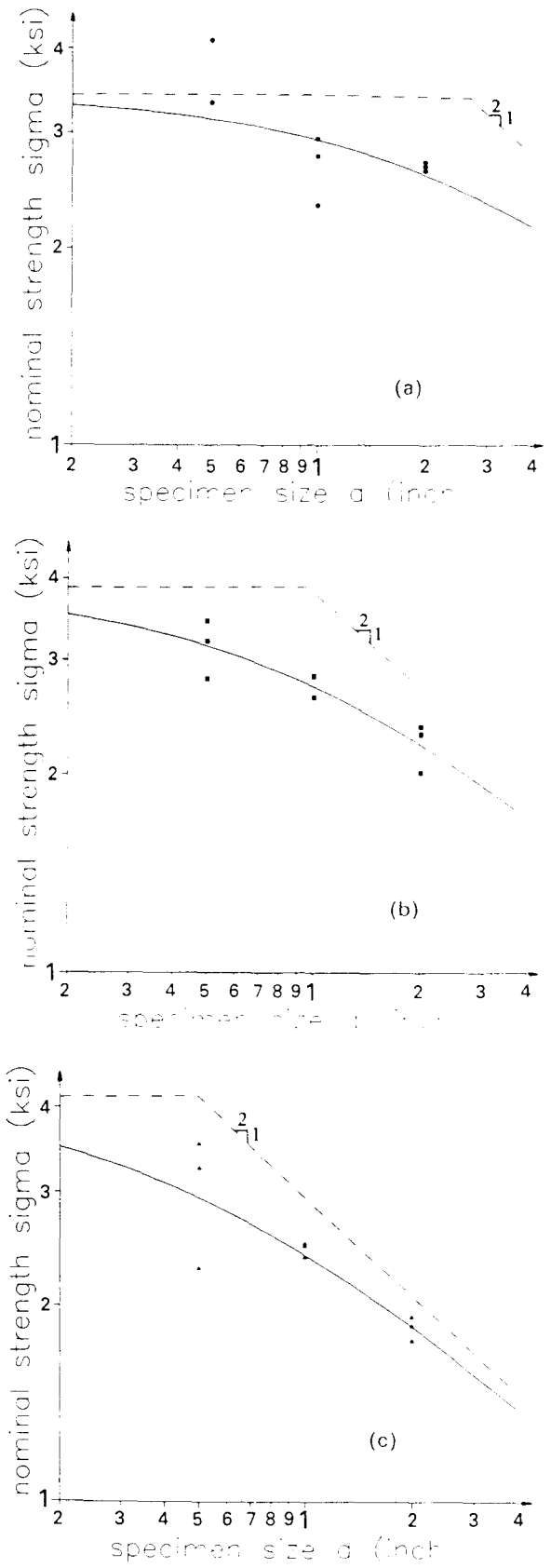

Fig. 10 Test results on size-effect plots for (a) small, (b) medium and (c) large slenderness.

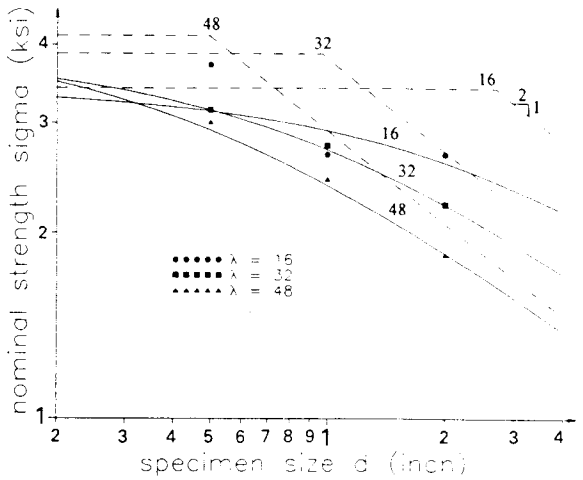

Fig. 11 Test results on size effect for all slendernesses . The slendernesses marked refer to columns without the end plates; 48, 32 and 16 correspond to actual slendernesses 52.5, 35.8 and 19.2.

axial splitting fracture. For the same reason, spiral columns will doubtless exhibit a weaker size effect than tied columns. The stronger the spiral, the weaker will be the size effect. For a concrete column encased in a very strong steel tube, the size effect will probably be eliminated because under very high triaxial confining pressures concrete becomes a plastic material, failing by frictional shear without softening.

The size effect in columns should be of particular concern for high-strength concrete, whose brittleness is notorious. Although the sound practice of using heavy spirals and steel tubes has been commonplace since the beginning, it is impossible to determine without appropriate experiments or fracture analysis what is precisely the minimum weight of steel tube that is needed to suppress the size effect and brittleness. Such a minimum required weight ought to be calculated rather than guessed, and for this fracture mechanics concepts are unavoidable.

6. CONCLUSIONS

Under the assumption that model tests on microconcrete adequately simulate the behaviour of columns made from concretes of normal aggregate size, and that bond slip has not contributed significantly to the size effect, the following conclusions may be drawn:

1. Tied reinforced concrete columns exhibit a strong size effect of fracture mechanics type.
2. The present test results are in agreement with the size effect law of Equation 5.
3. With increasing slenderness of the column, the size effect becomes stronger and the brittleness number increases.

In view of the fact that the size effect initially revealed by model tests of diagonal shear failures and anchor pull-out failures was subsequently verified by full-size tests, these conclusions most likely apply to columns made of normal concretes as well. This would mean that the safety margin for columns that are significantly larger than the majority of columns tested in laboratories in the past (by which the existing design codes were calibrated) will be significantly lower than that prescribed by the design code.

If, however, the observed size effect was caused primarily by bond slip, then the present results would not be fully relevant to real columns. The real columns are made of deformed reinforcing bars which offer much more resistance to slip. Further research in this regard in needed.

APPENDIX: Some related questions of scaling

Because of the empirically well-known effect of size of concrete test cylinders on their strength [15, 16] (for which an explanation has in the past been sought in statistics rather than fracture mechanics), a concrete experimentalist might argue that the concrete strength value $f'_c = 4200$ psi (28.95 MPa) measured on 3 in. (76 mm) companion cylinders is not representative of the concrete strength in $\frac{1}{2}$ in. (13 mm) thick model test columns. It must be emphasized, however, that this f'_c value is intended to serve merely as a characteristic of the concrete used, and *must not* be interpreted as the actual strength of the concrete in the test columns. That strength (i.e. the stress at which the column fails) can be quite different, because of several phenomena: (i) the difference in cross-section sizes of the columns and the companion cylinders, (ii) the partial confinement provided by the ties, (iii) the fact that bars promote axial splitting cracks along the bar surface, and (iv) generally the brittle or quasi-brittle failure cannot be characterized by strength alone anyway but is governed mainly by the rate of release of the stored strain energy (which is the essence of fracture mechanics, and is the primary inspiration for this study).

In view of the foregoing phenomena, using test cylinders of a small diameter such as 1 in. (25 mm) would not really be more relevant. Strictly speaking, the strength criterion is non-existent in the case of non-ductile failure.

As another variant of the foregoing objection, concrete experimentalists sometimes claim that for test cylinder diameters D exceeding 2 in. (50 mm) the size effect on strength disappears. The test results reproduced in Fig. A1 are offered to justify this claim ([15]; on the basis of this report, the use of a 2 in. diameter was recommended by this Committee). As a result, it has been taken for granted that the size effect seen in small-scale models of different sizes would not occur in normal-size structures.

This interpretation of test results, however, is deceptive. The supposed disappearance of size effect in compression for diameters above 2 in. (50 mm) is an illusion created by plotting the test results in the actual size scale, as shown in Fig. A1. Correctly, such plots should be made in logarithmic scales because, as is known from the theory of similitude [7], the scale effects normally follow power functions of size, which appear as straight lines in logarithmic scales. Fig. A1b shows the data from

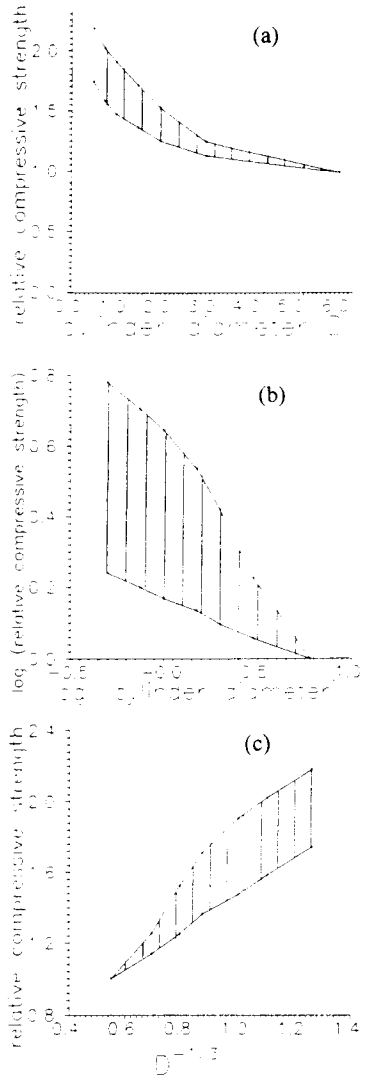

Fig. A1 Reanalysis of tests from ACI Committee 444 [15] for size effect on compression strength of model concretes.

Fig. A1a replotted in logarithmic scales, and Fig. A1c shows these data in the inverse power scale. We now see that these data in fact provide no basis at all for claiming that the size effect in the compression strength of test cylinders disappears for diameters above 2 in. (50 mm). The size effect, as seen in this plot, agrees very well with a power function of exponent $-\frac{1}{3}$, i.e. $f'_c \propto D^{-1/3}$ for these compression test data.

Another misconception persists with regard to the choice of the maximum aggregate size d_a in model tests. Some experimentalists might argue that the model columns of different sizes D should have been made with different aggregate sizes, with d_a proportional to D. Definitely not. If d_a were changed, one would have had a different concrete, with different properties. But the known scaling laws for geometrically similar structures of different sizes are valid only when one and the same material is used for all the sizes.

To understand the effect of changing the maximum aggregate size is of course important, too, but this study is concerned with the effect of structure size. The aggregate size effect is of a different nature. It is a complex materials science problem rather than a structural mechanics problem. Scaling the aggregate size would complicate evaluation of the test result and prevent isolating the structural size effect from other influences. From the structural engineer's viewpoint, the aggregate size effect is not a problem if the properties of the concrete to be used in the structure are known or specified.

In view of the effect of d_a, it should be realized that we are *not* trying to infer from the present tests the actual strength of full-size columns. We are only trying to ascertain how the strengths of columns of different sizes are mutually related. We find the relationship that holds among the model columns of different sizes made with reduced d_a, and then we infer that an approximately similar mutual relationship should hold among real columns of different sizes made with normal d_a. Unless full-size tests would prove such an inference to be invalid (which seems unlikely), responsible engineers cannot assume that the size effect revealed by the present tests does not exist in real columns, especially if it is known that the load–deflection curves of real columns, slender as well as stocky, do not end with a yield plateau but with a descending branch.

ACKNOWLEDGEMENTS

Partial financial support for the underlying theoretical studies of the size effect has been obtained under AFOSR Grant No. 91-0140 to Northwestern University, monitored by Dr J. Chang, and certain related size-effect studies were partly supported by the Center for Advanced Cement-Based Materials at Northwestern University. The second author wishes to express his gratitude for a fellowship from the Korean government supporting him during a one-year appointment as Visiting Scholar at Northwestern University. Thanks are due to Milan Jirásek, graduate research assistant, for his valuable comments and expert help in data evaluation after the second author returned to Korea, and also to technician John Chirayil for his expert assistance in the conduct of the tests.

REFERENCES

1. Bažant, Z. P., 'Should design codes consider fracture mechanics size effect?', in 'Concrete Design Based on Fracture Mechanics', edited by W. Gerstle and Z. P. Bažant, ACI Special Publication SP-134 (ACI, Detroit, 1992) pp. 1–23.
2. Bažant, Z. P. and Kwon, Y. W., 'Size effect in strength of reinforced concrete columns', in 'Fracture Mechanics of Concrete Structures', Proceedings of International Conference on Fracture Mechanics of Concrete Structures, Breckenridge, Colorado, June 1992, edited by Z. P. Bažant (Elsevier Applied Science, London, 1992), pp. 556–560.

3. Nilson, A. H. and Winter, G., 'Design of Concrete Structures', 10th Edn (McGraw-Hill, New York, 1986).
4. McGregor, J. G., 'Reinforced Concrete: Mechanics and Design' (Prentice-Hall, Englewood Cliffs, NJ, 1988).
5. Bažant, Z. P. and Cedloin, L., 'Stability of Structures: Elastic, Inelastic, Fracture and Damage Theories' (Oxford University Press, New York, 1991).
6. Bažant, Z. P., Cedolin, L. and Tabbara, M.R., 'New method of analysis for slender columns', *ACI Struct. J.* 88(4) (1991) 391–401.
7. Barenblatt, G. I., 'Dimensional Analysis' (Gordon and Breach, New York, 1987).
8. Bažant, Z. P., 'Size effect in blunt fracture: concrete, rock, metal', *J. Engng Mech. ASCE* **110** (1984) 518–535.
9. Bažant, Z. P., Xi, Y. and Reid, S. G., 'Statistical size effect in quasi-brittle structures: is Weibull theory applicable?', ibid. **117**(11) (1991) 2609–1622.
10. Bažant, Z. P. and Xi, Y., 'Statistical size effect in quasi-brittle structures: nonlocal theory', *ibid.* **117**(11) (1991) 2623–2640.
11. McGregor, J. G., Breen, J. E. and Pfrang, E. O. 'Design of slender columns', *ACI J. Proc.* **67**(1) (1970) 6–28.
12. Bažant, Z. P.and Kazemi, M. T., 'Determination of fracture energy, process zone length and brittleness number from size effect, with application to rock and concrete', *Int. J. Fract.* **44** (1990) 111–131.
13. Bažant, Z. P., 'Fracture energy of heterogeneous material and similitude', in 'Preprints of the SEM-RILEM International Conference on Fracture of Concrete and Rock', Houston, TX, edited by S. P. Shah and S. E. Swartz (Society for Experimental Mechanics, 1987) pp. 390–402.
14. Bažant, Z. P. and Pfeiffer, 'Determination of fracture energy from size effect and brittleness number', *ACI Mater. J.* **84** (1987) 463–480.
15. ACI Committee 444 (Models of Concrete Structures). 'Models of concrete structures: state-of-the-art', *Concrete International—Design and Constr.* **1**(1) (1979), 77–95.
16. Sabnis, G. M., Harris, H. G., White, R. N. and Mirza, M. S., 'Structural Modeling and Experimental Techniques' (Prentice-Hall, Englewood Cliffs, NJ, 1983).

RESUME

Ruine de poteaux de béton armé minces et de poteaux massifs: Essais d'effet d'échelle

On présente les résultats d'essais d'effet d'échelle sur des poteaux en béton armé. Ces poteaux, de grandeurs différentes, étaient homothétiques, avec des rapports de grandeurs 1:2:4 et des élancements de 19,2, 35,8 et 52,5. Ils avaient des sections carrées de 12,7, 25,4 et 50,8 mm, le pourcentage d'acier était de 4,91 et la dimension maximale du granulat de 3,2 mm. La charge présentait une excentricité égale à 0,25 de l'épaisseur du poteau. On a observé qu'il y avait un effet d'échelle remarquable à la charge de ruine, tel que la contrainte nominale à la ruine diminue quand la dimension augmente. Ce résultat contredit les réglementations selon lesquelles il n'y a pas d'effet d'échelle. Il faut en trouver l'explication dans la mécanique de la rupture fragile. Les résultats concordent avec la loi d'échelle proposée par Bažant. On trouve que, si l'élancement du poteau est plus grand, l'effet d'échelle augmente, de même que la fragilité de rupture caractérisant un comportement proche de celui décrit par la mécanique de la rupture fragile. Il reste à éclaircir le rôle joué par l'adhérence de l'acier.